

Probing of a Human Proteome Microarray With a Recombinant Pathogen Protein Reveals a Novel Mechanism by Which Hookworms Suppress B-Cell Receptor Signaling

Leon Tribolet,¹ Cinzia Cantacessi,^{1,5} Darren A. Pickering,¹ Severine Navarro,¹ Denise L. Doolan,² Angela Trieu,² Huang Fei,⁶ Yang Chao,⁶ Andreas Hofmann,³ Robin B. Gasser,⁴ Paul R. Giacomin,^{1,a} and Alex Loukas^{1,a}

¹Centre for Biodiscovery and Molecular Development of Therapeutics, Australian Institute of Tropical Health and Medicine, James Cook University, Cairns, ²QIMR Berghofer Medical Research Institute, and ³Eskitis Institute, Griffith University, Brisbane, and ⁴Faculty of Veterinary Science, University of Melbourne, Australia; ⁵Department of Veterinary Medicine, University of Cambridge, United Kingdom; and ⁶BGI-Shenzhen, China

***Na*-ASP-2 is an efficacious hookworm vaccine antigen. However, despite elucidation of its crystal structure and studies addressing its immunobiology, the function of *Na*-ASP-2 has remained elusive. We probed a 9000-protein human proteome microarray with *Na*-ASP-2 and showed binding to CD79A, a component of the B-cell antigen receptor complex. *Na*-ASP-2 bound to human B lymphocytes *ex vivo* and downregulated the transcription of approximately 1000 B-cell messenger RNAs (mRNAs), while only approximately 100 mRNAs were upregulated, compared with control-treated cells. The expression of a range of molecules was affected by *Na*-ASP-2, including factors involved in leukocyte transendothelial migration pathways and the B-cell signaling receptor pathway. Of note was the downregulated transcription of *lyn* and *pi3k*, molecules that are known to interact with CD79A and control B-cell receptor signaling processes. Together, these results highlight a previously unknown interaction between a hookworm-secreted protein and B cells, which has implications for helminth-driven immunomodulation and vaccine development. Further, the novel use of human protein microarrays to identify host–pathogen interactions, coupled with *ex vivo* binding studies and subsequent analyses of global gene expression in human host cells, demonstrates a new pipeline by which to explore the molecular basis of infectious diseases.**

Keywords. hookworm; *Necator americanus*; *Na*-ASP-2; SCP/TAPS; CD79A; B cell; antigen receptor; protein microarray; host–pathogen interaction.

The hookworm *Necator americanus* is one of the most prevalent pathogens of humans, infecting 576–740 million people worldwide [1]. Hookworms can persist for many years within their hosts [2], having evolved a suite of strategies to evade immune attack, from the point of percutaneous entry and pulmonary migration

by third-stage larvae (L3) through their final site of residence as adult worms in the gut. While hookworm infection can be treated with anthelmintic drugs, reinfection rapidly occurs [3], precipitating an urgent need for development of vaccines to limit the global burden of human hookworm infections [4].

Efforts to develop vaccines against hookworm infection have focused on discovery of antigens secreted by the L3 stage. Serum antibodies from dogs vaccinated with irradiated hookworm L3 [5] and people from hookworm-endemic areas with high antibody titers but low egg counts [6] predominantly recognize members of the activation-associated protein (ASP) family, notably *Na*-ASP-2. In a phase 1a vaccine trial in hookworm-naïve subjects from the United States, recombinant *Na*-ASP-2 was well-tolerated and immunogenic

Received 24 May 2014; accepted 31 July 2014; electronically published 19 August 2014.

^aP. R. G. and A. L. contributed equally to this report.

Correspondence: Alex Loukas, PhD, Australian Institute of Tropical Health and Medicine, QTHA Bldg E4, James Cook University, McGregor Rd, Smithfield, QLD 4878, Australia (alex.loukas@jcu.edu.au).

The Journal of Infectious Diseases® 2015;211:416–25

© The Author 2014. Published by Oxford University Press on behalf of the Infectious Diseases Society of America. All rights reserved. For Permissions, please e-mail: journals.permissions@oup.com.

DOI: 10.1093/infdis/jiu451

[7]. However, a phase 1b trial in hookworm-exposed individuals in Brazil was halted because of the development of urticarial reactions in people with preexisting immunoglobulin E (IgE) against *Na*-ASP-2 [8]. Despite the safety concerns, there remains interest in *Na*-ASP-2 as a vaccine candidate, particularly if it used as a pediatric vaccine prior to the development of anti-hookworm IgE responses or if it is modified to reduce its allergenic capacity [9], which has proven effective for peanut, dust mite, and wasp allergens [10–12].

Despite the relatively long history of research into hookworm ASPs as vaccines, relatively little is known about their biological roles. ASP-2 is one of the most abundant excretory/secretory (ES) proteins produced by L3 upon exposure to host serum [13, 14]. However, its expression is diminished as the parasite migrates through the lung, provoking the hypothesis that ASP-2 may be involved in immune regulation while the parasite resides in the circulatory system. Administration of recombinant *Na*-ASP-2 to rodents elicits a type 2 cytokine response, robust antibody production, and neutrophil recruitment [5, 15], although direct interactions between *Na*-ASP-2 and a defined cell type were not elucidated. The hookworm ASP protein family forms 3 distinct structural groups, based on X-ray crystallographic studies [16, 17]. The crystal structure of *Na*-ASP-2 indicates the presence of a putative electronegative binding cavity flanked by conserved His and Glu residues [17], suggesting that an unknown ligand or binding partner exists. Another hookworm-derived ASP-like protein, neutrophil inhibitory factor, has been shown to directly interact with host CD11b, thereby inhibiting neutrophil function [18]. Thus, it remains likely that *Na*-ASP-2 binds to a cell surface receptor from its human host to exert its effector function(s).

Herein we describe the first probing of a human proteome microarray with a pathogen-derived protein to reveal a selective interaction between *Na*-ASP-2 and CD79A, a component of the B-cell antigen receptor complex. We confirm the interaction by showing that *Na*-ASP-2 binds to human B cells *ex vivo* and triggers changes in expression of B-cell–intrinsic genes, notably those encoding key signaling molecules of the antigen receptor pathway.

METHODS

Ethics

Healthy white volunteers (aged 30–45) from Cairns, Australia, a region that is not endemic for human hookworm infection, were used as a source of peripheral blood under informed consent using a protocol (H4385) approved by the James Cook University Human Research Ethics Committee.

Probing of a Human Protein Microarray with Recombinant *Na*-ASP-2

Purified, full-length recombinant *Na*-ASP-2 was a kind gift from Dr Bin Zhan (Baylor College of Medicine, Houston,

TX). The protein was expressed in *Pichia pastoris* and purified via 2 ion exchange chromatography steps, followed by a final desalting step as described elsewhere [19]. *Na*-ASP-2 was biotinylated with NHS-LC-biotin (Thermo-Fisher) and used to probe a Human V5 ProtoArray (Invitrogen) at a final concentration of 50 µg/mL. The ProtoArray contains >9000 human proteins printed in duplicate and includes >2600 membrane proteins. Binding of biotinylated *Na*-ASP-2 to proteins on the array was detected with streptavidin Alexa Fluor 647 at a 1:1000 dilution in Protoarray blocking buffer (Invitrogen). The array was scanned using a GeneArray 4000B scanner (Molecular Devices) at 635 nm. Results were saved as a multi-TIFF file and analyzed using Genepix Prospector software, version 7.

Molecular Modeling

Comparative modeling was used to generate a 3-dimensional atomic model of human CD79A, using the crystal structure of human CD79B (PDB accession code 3kg5) as a template. A secondary structure–based amino acid sequence alignment of CD79A and CD79B was prepared with SBAL [20] and used to guide the comparative modeling calculations. Twenty independent models were calculated with MODELLER [21], and the one with the lowest energy was selected and superimposed onto one of the monomers in the CD79B homodimer structure (rigid body modeling). The secondary structure topology and amino acid sequence of CD79A is compatible with the intermolecular interactions observed in the CD79 homodimer structure [22]. A minor manual adjustment was made to enable intermolecular disulphide bond formation (CysA119–CysB136) in the resulting heterodimer. Both cysteine residues were in prime position for this bond, which is also observed in the CD79B homodimer. The crystal structure of *Na*-ASP-2 was docked to the CD79 heterodimer model, using a rigid body approach based on a multidimensional spherical polar Fourier correlation with shape and electrostatics expansion as implemented in Hex [23]. The rigid body docking calculations were performed without preferred contacts to enable an unbiased complex formation. From the generated 100 independent models, the highest scoring one (energy score, –873; next highest energy score, –720) was chosen. The figures were generated with PyMOL [24].

Blood Lymphocyte Isolation and Culture

Human peripheral blood mononuclear cells (PBMCs) were isolated by density centrifugation (Lymphoprep). Cells (1×10^6 cells mL⁻¹) were incubated for 4 or 24 hours at 37°C in either 96-well plates (for flow cytometry) or 24-well plates (for sort purification) with *Na*-ASP-2 in Dulbecco's modified Eagle's medium with 10% heat-inactivated fetal bovine serum, 2 mM L-glutamine, 100 U/mL penicillin, 100 U/mL streptomycin, and 25 mM HEPES (medium). B-cell activation was

induced by stimulation with 10 µg/mL of goat F(ab')₂ anti-human immunoglobulin M (IgM; µ chain; Sigma) for 24 hours.

Flow Cytometry and Cell Sorting

Cells were stained with fluorophore-conjugated antibodies against CD19 (HIB19), CD20 (2H7), CD3 (OKT3), CD4 (OKT4), CD14 (61D3) CD69 (FN50), HLA-DR (LN3), CD80 (2D10.4), and CD86 (IT2.2), all of which were from eBioscience. In experiments using biotinylated *Na*-ASP-2, streptavidin–fluorescein isothiocyanate (FITC) was included in the staining panel. Cells were analyzed using a BD-FACSCanto II flow cytometer. Alternatively, CD3[−]CD14[−]CD19⁺CD20⁺ cells were sort purified by using a BD-FACSAria III cell sorter.

RNA Isolation

RNA was extracted from sort-purified CD19⁺CD20⁺ B cells for high-throughput RNA sequencing at BGI (Hong Kong) or for real-time quantitative polymerase chain reaction (qPCR) analysis. Pelleted cells were lysed in RLT buffer (Qiagen) plus beta-mercaptoethanol and stored at −80°C until RNA was extracted using the RNeasy kit with DNase purification (Qiagen). The concentration and integrity of each RNA preparation were verified on a 2100 Bioanalyzer (Agilent), and each preparation was stored in RNastable tubes (Biomatrix) at room temperature until subsequent use.

Illumina Sequencing

RNA underwent reverse transcription to complementary DNA (cDNA) using the Illumina TruSeq sample preparation kit. Briefly, 1.0 µg of total RNA from each cell preparation was used for poly-A mRNA selection using streptavidin-coated magnetic beads. Two rounds of poly-A mRNA enrichment were performed, followed by thermal fragmentation of the mRNA to a length of 100–500 bp. Each fragmented RNA sample underwent reverse transcription to cDNA by using random primers, underwent end repair, and underwent adaptor ligation (Illumina). Ligated products were amplified by PCR (15 cycles) and were cleaned using a MinElute column (Qiagen). Amplicons underwent paired-end sequencing on an Illumina HiSeq 2500 (Illumina).

Bioinformatics Analyses

Ninety-base pair single-reads were screened for the presence of adapter sequences and sequences with >10% unknown bases and sequences with >50% low-quality bases. The remaining reads underwent splice alignment with the human genome reference assembly GRCh37 (National Center for Biotechnology Information [NCBI] build 37.1), using TopHat, which incorporates the Bowtie v0.11.3 algorithm [25]. Subsequently, individual aligned read files were assembled into transcripts, using Cufflinks [26]. Relative levels of transcription were measured using the reads per kilobase per million (RPKM) algorithm [27]. Differences in levels of gene transcription were determined

as previously described [28]. The false discovery rate method (FDR) [29] was used to correct the errors associated with multiple pairwise comparisons ($FDR \leq 0.001$), and a log₂ ratio with an absolute value of ≥ 1 was set as the threshold for the significance of gene expression changes. Differentially expressed genes (DEGs) were mapped to Gene Ontology terms and Kyoto Encyclopedia of Genes and Genomes (KEGG) biological pathways available in the GO (<http://www.geneontology.org>) and KEGG (<http://www.genome.jp/kegg/>) databases, respectively. A hypergeometric test was subsequently used to identify GO terms and KEGG pathways in DEGs that were significantly enriched, compared with the transcriptome background, using the GOTerm: Finder software [30]. The calculated *P* values were subjected to Bonferroni correction using the corrected *P* value of .05 as a threshold. Raw sequence data have been deposited in the Sequence Read Archive (SRA) of NCBI under BioProject accession ID PRJNA259640.

Real-Time qPCR

Total RNA was extracted from sort-purified B cells, obtained from 4 hookworm-naive white human volunteers, that were cultured for 24 hours in the presence or absence of *Na*-ASP-2. cDNAs were prepared using Superscript III reverse transcriptase (Invitrogen). SYBR Green Master Mix (Qiagen) was used with a Rotor-Gene q thermal cycler (Qiagen). The oligonucleotides were designed manually and synthesized (Integrated DNA Technologies). Data were analyzed using the $\Delta\Delta$ CT method, whereby actin served as the endogenous gene and samples were normalized to medium controls. Primer sequences were as follows: *β-actin*, ATTGGCAATGAGCGGTTC (forward) and GGATGCCACAGGACTCCAT (reverse); *lyn*, GAGACTCGGGGAGCCATTG (forward) and ACGCTGGGGATGTTA TACTCT (reverse); and *pi3kr5* (23 533), CTTCCACGCTAC GTGTTGTG (forward) and TGAAGTTTGAAGAACCGT GTGAG (reverse).

Statistical Analyses

Statistical analyses of qPCR data were conducted using a paired *t* test in which $\Delta\Delta$ CT values for each gene of interest were compared between test (*Na*-ASP-2 exposed) and control (medium exposed) cells. *P* values of <.05 were deemed statistically significant.

RESULTS

Interaction Between *Na*-ASP-2 and Human CD79A Revealed by Probing of a Human Proteome Microarray

Probing of the human proteome array with biotinylated *Na*-ASP-2 revealed interactions between *Na*-ASP-2 and 5 human proteins. The strongest interaction was with propionyl-CoA carboxylase (PCCA), an anticipated interaction because PCCA is a biotin-binding enzyme and would therefore be

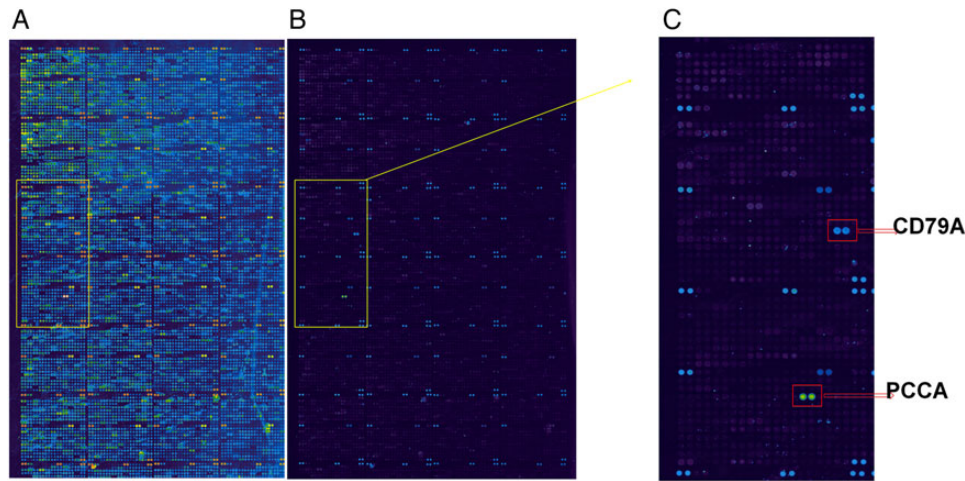


Figure 1. Binding of biotinylated *Na*-ASP-2 to CD79A and biotin-binding proteins on a Human V5 ProtoArray. The array was probed with biotinylated recombinant *Na*-ASP-2 followed by streptavidin Alexa Fluor 647 and scanned with a GeneArray 4000B scanner at 635 nm, using laser intensity settings of 100% (A) and 66% (B). Yellow boxes denote the area of the array containing duplicate spots of CD79A and PCCA. A magnified view of the area contained within the yellow boxes is also shown (C). All other spots are positive control proteins spotted in duplicate to allow orientation on the array. Two separate arrays were probed independently, with representative results from 1 experiment displayed.

expected to bind to any biotinylated recombinant protein used to probe the array (Figure 1, Supplementary Table 1). Indeed, we have noted consistent binding of other (unrelated) biotinylated recombinant proteins to PCCA (unpublished data). The second most intense association was with CD79A, which, together with CD79B, forms a heterodimer and a subunit of the B-cell antigen receptor. The third and fifth strongest hits were also proteins involved in biotin metabolism (Supplementary Table 1). The fourth strongest association was with cortactin, which is involved in actin remodeling and was of sufficiently low signal intensity (2.4-fold lower than CD79A) that we deemed it unworthy of further pursuit (Supplementary Table 1). Probing of a second array under identical conditions resulted in consistent binding between *Na*-ASP-2 and the same 5 human proteins on the array.

Modeling of *Na*-ASP-2 Interactions with CD79

We recently panned a random 12-mer peptide phage display library with *Na*-ASP-2 and showed that most of the bound peptides were enriched for glutamine and histidine residues [31]. Interestingly, the extracellular domain of CD79A contains a HXQXXH motif at residues 51–56. This peptide forms part of a large surface of CD79A, which has previously been implicated in binding of the B-cell antigen receptor [22]. Rigid body docking of the crystal structure of *Na*-ASP-2 and a model of heterodimeric CD79A/CD79B suggests that, on the basis of shape and electrostatics data, *Na*-ASP-2 may bind to the CD79 heterodimer (Figure 2). Furthermore, this model indicates that *Na*-ASP-2 mainly interacts with the CD79A surface harboring the HXQXXH motif, but a protruding loop of CD79B (residues 79–86) may also engage in interactions with the hookworm protein.

Na-ASP-2 Binds Selectively to Human B Cells

CD79A is expressed exclusively on B lymphocytes. To verify the interaction between *Na*-ASP-2 and CD79A, we cultured human PBMCs from healthy, hookworm-naive human volunteers *ex vivo* for 4 or 24 hours with biotinylated *Na*-ASP-2 and performed flow cytometry. Cells were stained for B-cell markers (CD19 and CD20), T-cell marker CD3, monocyte marker CD14, and streptavidin-FITC for detection of surface-bound *Na*-ASP-2. This experiment was performed twice, with 2 different blood donors. As expected, we detected negligible frequencies of FITC⁺ cells following treatment with medium or nonbiotinylated *Na*-ASP-2. However, treatment with increasing amounts of biotinylated *Na*-ASP-2 resulted in a dose-dependent increase in the frequency of *Na*-ASP-2/FITC⁺ cells (Figure 3A). Gated FITC⁺ cells were analyzed for various leukocyte surface markers. While only 8% of FITC⁺ cells expressed CD3 or CD14, the majority (72%) of FITC⁺ cells coexpressed CD20 and CD19, a phenotype consistent with human B lymphocytes (Figure 3B). Modifying culture time, temperature, and cell permeabilization state did not enhance the detection of FITC⁺ cells (data not shown), but in each case, B cells represented the dominant *Na*-ASP-2/FITC⁺ population.

Na-ASP-2 Induces Substantial Changes in B-Cell Gene Expression

To examine the biological effect of *Na*-ASP-2 on human B cells, we compared the expression of cell activation markers following polyclonal stimulation of the B-cell receptor. PBMCs were treated for 4 hours with 2 μg/mL *Na*-ASP-2 or bovine serum albumin control and stimulated for 24 hours with either medium or anti-human IgM. While we did not observe appreciable

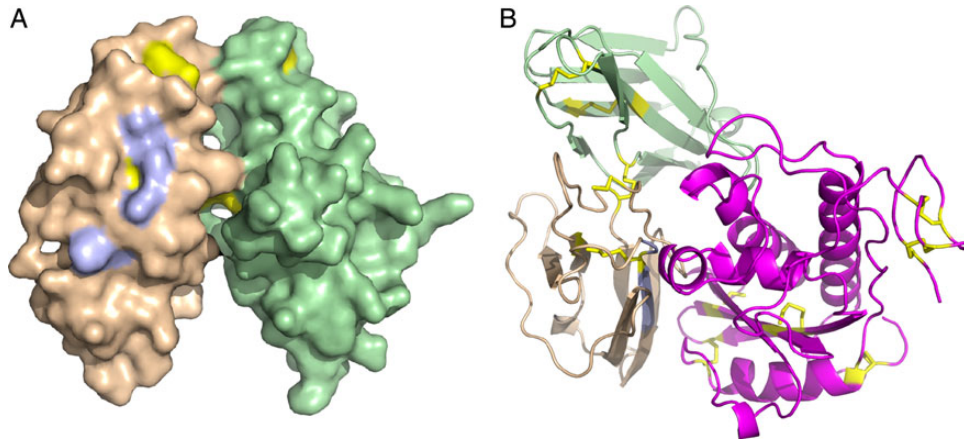


Figure 2. Rigid body models of the CD79A/CD79B heterodimer (A) and the CD79A/CD79B:Na-ASP-2 complex (B). CD79A is colored wheat; CD79B, pale green; and Na-ASP-2, magenta. Cysteine residues and disulphide bonds are rendered as sticks in yellow. The CD79A peptide HFQCPH (residues 51–56) is colored blue. A, Surface representation of the CD79 heterodimer model. B, Cartoon rendering of the modeled ternary complex of Na-ASP-2 and CD79.

differences in the expression levels of CD69, CD86, HLA-DR, and CD80 on B cells exposed to Na-ASP-2 following anti-IgM treatment, we did observe slight but consistent reductions in expression of these markers when cells underwent no exogenous stimulation (Supplementary Figure 1). These data suggest that B cells can still be activated in the presence of Na-ASP-2

but that, in the absence of polyclonal stimulation, Na-ASP-2 may limit the activation state of human B cells.

To investigate the cascade of molecular events that follow binding of Na-ASP-2 to human B cells, we performed sort purification on CD19⁺CD20⁺ B cells from one volunteer's whole PBMC culture that was treated with either Na-ASP-2

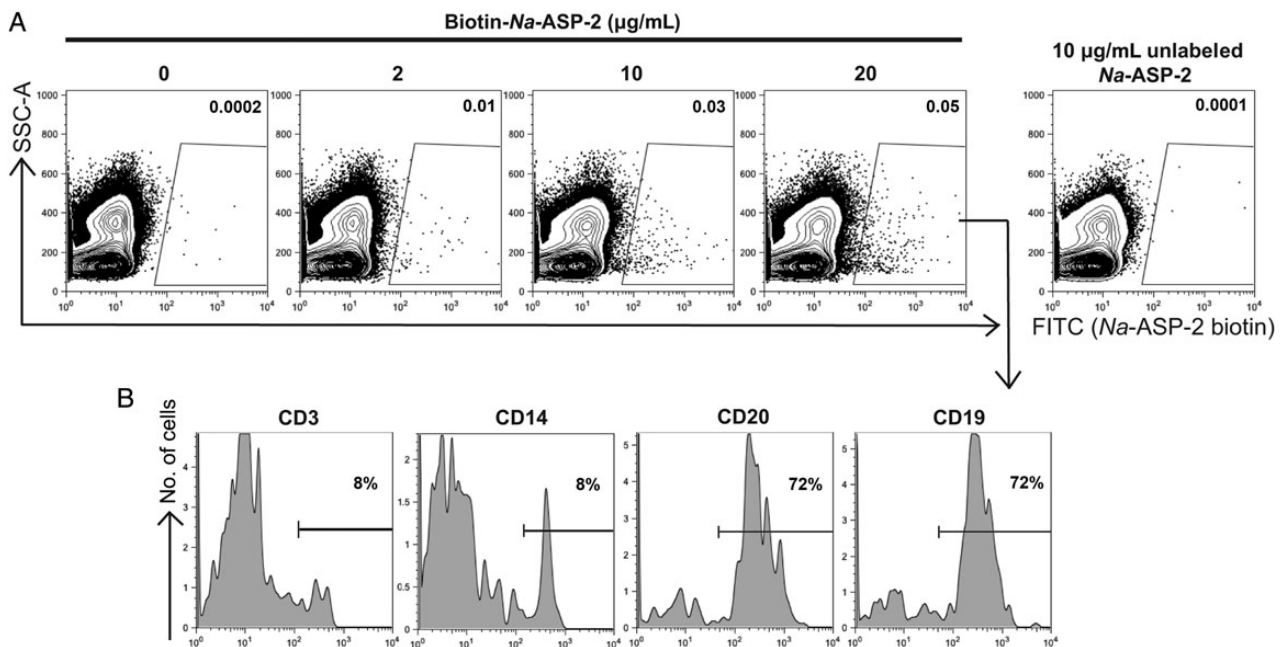


Figure 3. Na-ASP-2 binds selectively to human B-cells. Peripheral blood mononuclear cells from hookworm-naïve donor volunteers were cultured for 24 hours in the presence of increasing concentrations of biotinylated recombinant Na-ASP-2 or with unlabeled Na-ASP-2. A, Frequencies of cells with biotinylated Na-ASP-2 on the surface were quantified by flow cytometry after incubation with fluorescein isothiocyanate (FITC)-conjugated streptavidin. B, Na-ASP-2⁺ FITC⁺ cells were gated for analysis of the immune cell-surface markers CD3, CD14, CD20, and CD19. Experiments were conducted twice, with 2 different blood donors. Representative data are shown.

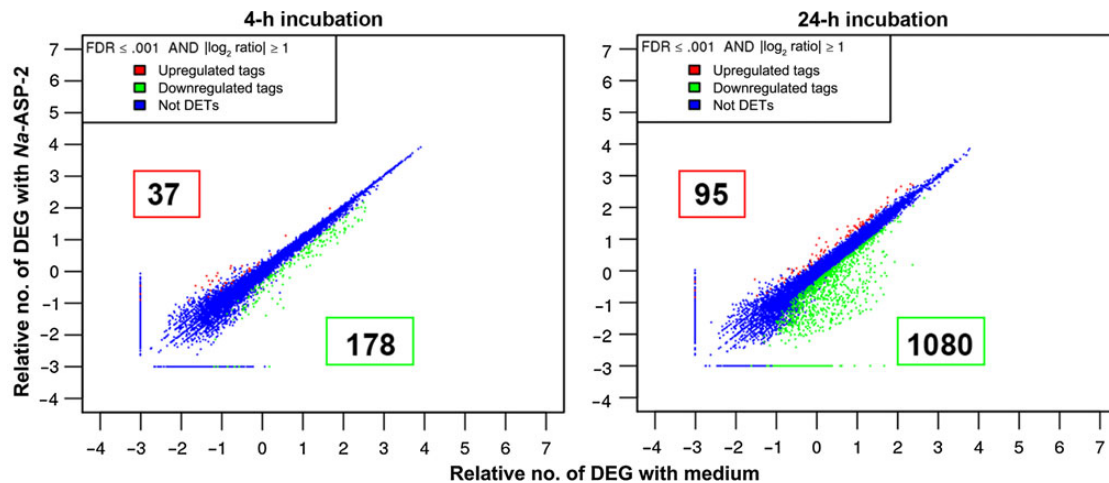


Figure 4. Changes in messenger RNA expression in B cells from a hookworm-naive human volunteer after culture with *Na-ASP-2*. Peripheral blood mononuclear cells were cultured for 4 or 24 hours with either medium or 2 $\mu\text{g}/\text{mL}$ *Na-ASP-2*; CD19⁺ CD20⁺ B cells underwent sort purification, and isolated RNA was subjected to RNA sequencing analysis. Scatter plots comparing \log_2 ratios of reads per kilobase per million expression values for B cells obtained from a hookworm-naive human volunteer following ex vivo coculture with *Na-ASP-2* at 4 and 24 hours. Numbers indicate the numbers of upregulated or downregulated genes. Abbreviations: DEGs, differentially expressed genes; DETs, differentially expressed transcripts; FDR, false discovery rate.

or medium control and then performed RNA-Seq and bioinformatics analyses. B cells that were cultured with *Na-ASP-2* for 4 hours underwent minimal changes in gene expression (37 upregulated genes and 178 downregulated genes, compared with medium control; Figure 4A). After 24 hours of culture, however, there was a pronounced bias toward downregulation of gene expression in B cells that were cultured with *Na-ASP-2*, with 1080 significantly downregulated genes and only 95 upregulated genes (Figure 4B).

***Na-ASP-2* Downregulates Expression of Genes Involved in Multiple Biological Pathways**

Genes whose expression was significantly altered following exposure to *Na-ASP-2* were clustered according to their KEGG annotation (Figure 5). In particular, the majority of downregulated genes could be mapped to the cytokine-cytokine receptor interaction (ko04060) and the leukocyte transendothelial migration (ko04670) pathways, whereas the majority of genes whose expression was upregulated by *Na-ASP-2* binding could be mapped to the hematopoietic cell lineage (ko04640) and chemokine signaling pathway (ko04062), respectively.

***Na-ASP-2* Downregulates Expression of Genes in the Immunoglobulin Receptor (CD79A) Signaling Pathway**

While *Na-ASP-2* appears to affect the expression of genes involved in multiple biological pathways, we focused on potential consequences of interactions between *Na-ASP-2* and CD79A, based on our earlier protein-protein interaction studies. In particular, 3 genes mapping to the KEGG B-cell receptor signaling pathway: *lyn*, spleen tyrosine kinase (*syk*), and phosphatidylinositol

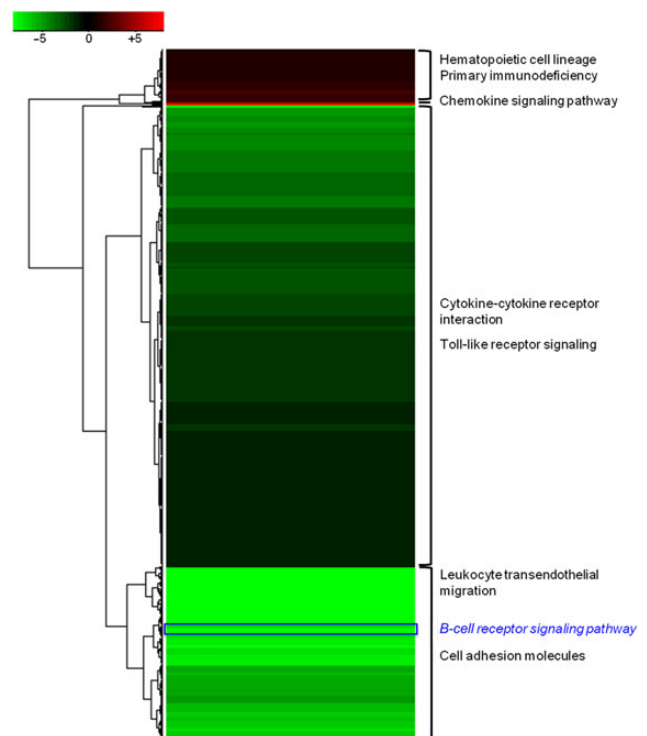


Figure 5. Differential gene expression following 24-hour exposure to *Na-ASP-2*. Heat map analysis of differentially expressed genes following 24 hours culture of sort-purified human B cells with *Na-ASP-2*. Differentially expressed genes are clustered according to their Kyoto Encyclopedia of Genes and Genomes (KEGG) annotation (<http://www.genome.jp/kegg/>). The top KEGG pathways assigned to the majority of genes within each cluster are also reported.

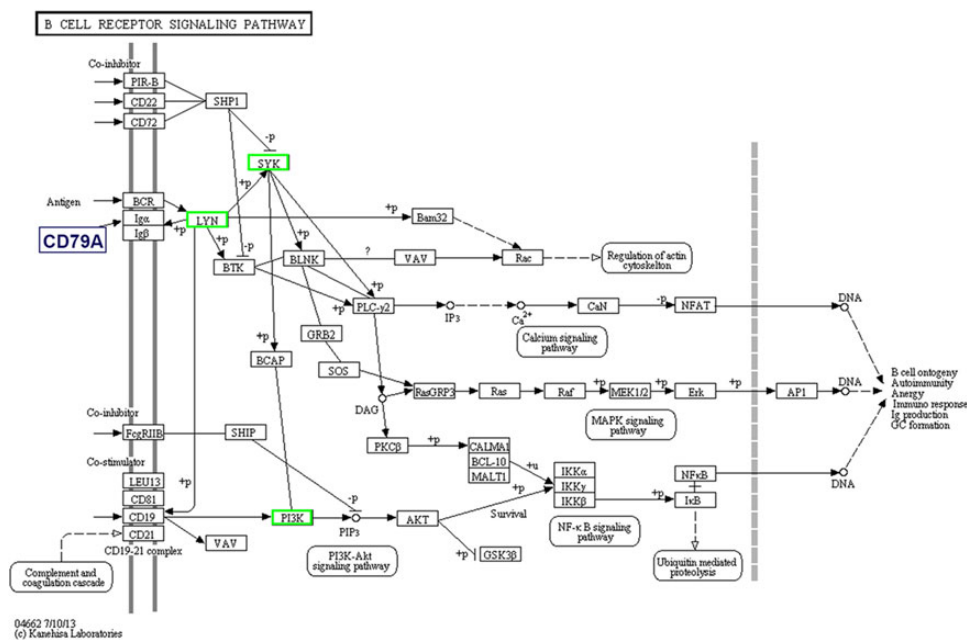


Figure 6. *Na*-ASP-2 causes B-cell–intrinsic reductions in expression of messenger RNAs immediately downstream of CD79A. Schematic representation of the B-cell receptor signaling pathway (modified from http://www.genome.jp/kegg-bin/show_pathway?hsa04662). Genes whose expression was downregulated following 24-hour coculture of B cells with *Na*-ASP-2 are indicated by green boxes.

3-kinase (*pi3k*) displayed significant downregulation following exposure to *Na*-ASP-2 (Figure 6). Each of these gene products are involved in transmitting signals from the B-cell receptor and are crucial for essential B-cell functions, such as activation, development, proliferation, inhibition, and cell death.

Follow-up studies involving the analysis of B-cell–intrinsic gene expression induced by *Na*-ASP-2 from 4 hookworm-naive blood donors were performed using qPCR. Consistent with our findings from RNA sequencing analysis, the expression levels of both *lyn* and *pi3k* were significantly reduced in B cells that were cultured for 24 hours with *Na*-ASP-2 ex vivo relative to control cells (Figure 7).

DISCUSSION

Advances in genomics and proteomics have served to highlight how little we know about the functional interactions of parasitic helminth proteins with their respective hosts tissues [32]. Approaches aimed at developing a portfolio for a specific pathogen protein of unknown function have provided information on expression, localization, and immunogenicity [33]. None of these approaches, however, specifically addresses biochemical function or ligand/receptor interactions. The ES proteins of helminths from diverse phyla have been characterized using proteomics. However, despite the availability of draft genomes for some of these organisms, >50% of genes encoding secreted proteins remain functionally uncharacterized. This is true for *N. americanus*, in which 33% of the

genome encodes for putatively secreted proteins but >30% remain unannotated [34].

N. americanus modulates the human host's immune system to facilitate its migration from the skin to the lungs en route to the intestine [35]. Immunoepidemiological studies from human populations have shown that protective acquired immunity to hookworm does not develop in most individuals [36]. One of the means by which hookworms modulate the host's immune system is via the production of ES proteins [37–40]. Consistent with this theory are the results from our study, in which we demonstrated that *Na*-ASP-2 interacts with CD79A on human B lymphocytes, suppressing expression of genes that play key roles in multiple biological pathways, including the B-cell receptor signaling pathway. While the precise biological function of *Na*-ASP-2/B-cell interactions in vivo remains unclear, our in vitro data imply that *Na*-ASP-2 engages CD79A and results in suppression of molecules that determine the activation state of B cells. Our findings neither support nor contradict those of Bower et al [15], who showed that *Na*-ASP-2 recruits neutrophils. While neutrophils are essential effector cells in acute infections, they also suppress B-cell and T-cell responses by competing for antigen with professional antigen-presenting cells [41]. Moreover, neutrophils indirectly regulate dendritic cell and T-cell interactions [42]. Therefore, *Na*-ASP-2 might serve to suppress immune responses via 2 distinct but convergent pathways.

In the absence of experimental 3-dimensional structures of *Na*-ASP-2 in complex with host proteins, we generated a

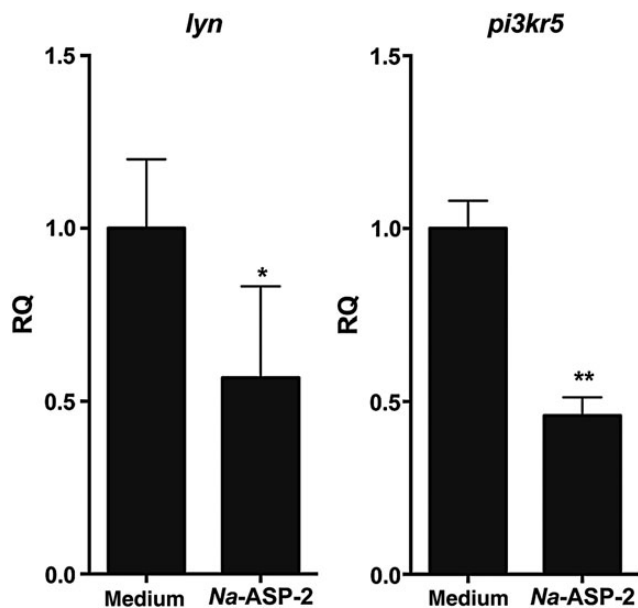


Figure 7. Downregulated expression of *lyn* and *pi3kr5* in human B-cells from 4 hookworm-naive human volunteers after culture with *Na-ASP-2*. Peripheral blood mononuclear cells from 4 hookworm-naive donor volunteers were cultured for 24 hours in the presence of medium alone or 2 $\mu\text{g}/\text{mL}^1$ recombinant *Na-ASP-2*. Quantitative polymerase chain reaction analysis of *lyn* and *pi3kr5* was performed on RNA derived from sort-purified B-cells. Data were analyzed using the $\Delta\Delta\text{CT}$ method, whereby actin served as the endogenous gene and samples were normalized to medium controls. * $P = .0295$ and ** $P = .0004$. Abbreviation: RQ, relative quantification.

model of the *Na-ASP-2*:CD79A:CD79B heterotrimer complex. This model is in agreement with 2 previously reported findings. First, the interaction interface between the hookworm protein and the CD79 heterodimer has a His/Gln-containing motif with similar properties to those identified by panning a random peptide library with *Na-ASP-2* [31]. Second, the vast majority of the interaction interface of *Na-ASP-2* and CD79 is on the α -subunit, coinciding with the interaction interface of CD79 with membrane immunoglobulin [22]. We recently identified the human SK3 channel as a putative receptor of *Na-ASP-2* on the basis of the presence of a His/Gln-rich peptide that interacted with *Na-ASP-2* in vitro [31]. Since this His/Gln peptide sequence is only present in one of the isoforms of the SK3 channel (isoform 1), and the human V5 ProtoArray included isoform 2, no interactions with SK3 were observed in this study.

The human B-cell receptor consists of a 1:1 stoichiometry of membrane-bound immunoglobulin and CD79A/CD79B. The immunoglobulin domain relies on a noncovalent association with the CD79A/CD79B heterodimer complex for triggering a signaling cascade [43]. Upon binding of antigen to membrane-bound immunoglobulin, the receptor complex undergoes conformational changes, resulting in recruitment of LYN, phosphorylation of the relevant CD79 tyrosines, PI3K recruitment to

CD19 and adaptor proteins, and generation of the potent lipid secondary messenger phosphatidylinositol 3,4,5-trisphosphate (PIP3). How interactions between CD79A and *Na-ASP-2* result in downregulated expression of *lyn* and *pi3kr5* is unclear, but it is possible that *Na-ASP-2* may induce an anergic-like state in B cells by preventing B-cell receptor clustering and activation of the cell upon antigen binding. Anergic B cells are characterized by impaired propagation of activating signals that are triggered by CD79 engagement [44], have substantially reduced PIP3 production [45], and have a dramatically reduced life span. While *Na-ASP-2* does not limit the capacity for B cells to be activated by polyclonal stimulation, the activation state of resting B cells appeared to be lowered. Further studies are required to determine whether *Na-ASP-2* can regulate the B-cell-intrinsic responses to more physiologically relevant antigens, particularly ES proteins. Hookworms are known to induce a state of immune hyporesponsiveness in chronic infections [36, 46], and by probing a hookworm protein microarray [34] we found that the most heavily infected individuals generated lower IgG responses than did individuals with low or moderate intensity infections (S. Gaze and A. Loukas, unpublished data). These findings serve to highlight the altered B-cell functions in individuals with heavy hookworm infection and offer a potential causative role for proteins such as *Na-ASP-2*. However, this hypothesis requires rigorous testing, potentially in well-controlled hookworm dose-ranging studies [47].

To our knowledge, this is the first report of a pathogen protein that interacts with the B-cell receptor or modulates expression of signaling molecules that determine B-cell function. Given the interest in hookworm-secreted proteins for treating autoimmune and allergic diseases [40, 48], our findings suggest that *Na-ASP-2* warrants testing as a novel biologic for treating B-cell-mediated autoimmunity. Administration of anti-CD79 or anti-CD79B monoclonal antibodies prevent collagen-induced arthritis [49] or lupus [50], respectively, in mice, offering the potential for reduced side effects while maintaining B cells in a transient anergic state that does not require their depletion. Thus, *Na-ASP-2* could prove beneficial as a treatment for autoimmune B-cell-mediated diseases, such as multiple sclerosis or rheumatoid arthritis.

Our findings herein highlight the novel application of protein microarray technology to address host-hookworm interactions at the protein level and provide a powerful and rapid screening process that could be applied to the study and identification of interactions between other pathogens and host proteins. By coupling the probing of the human proteome array with *in vivo* confirmation of binding to live cells and subsequent NGS to determine changes in gene expression, we have demonstrated the usefulness of this pipeline for elucidating novel host-pathogen interactions and assigning functions to that enigmatic group of pathogen molecules that are frustratingly referred to as “proteins of unknown function.”

Supplementary Data

Supplementary materials are available at *The Journal of Infectious Diseases* online (<http://jid.oxfordjournals.org>). Supplementary materials consist of data provided by the author that are published to benefit the reader. The posted materials are not copyedited. The contents of all supplementary data are the sole responsibility of the authors. Questions or messages regarding errors should be addressed to the author.

Notes

Acknowledgments. We thank Drs Peter Hotez, Maria Elena Bottazzi, Bin Zhan, Soraya Gaze, Travis Beddoe, and Phil Felgner, for helpful discussion and provision of reagents.

Financial support. This work was supported by the Australian Research Council (Linkage Project grant 100100092 to R. B. G., A. H., and A. L.); the National Health and Medical Research Council (NHMRC; Program Grant 1037304 to A. L. and D. L. D.; NHMRC Overseas Biomedical Fellowship 613718 to P. G.; NHMRC Early Career Research Fellowship 1052936 to C. C.; and NHMRC Principal Research Fellowships 1020114 to A. L. and 1023636 to D. L. D.); the Victoria Life Sciences Computation Initiative (VLSCI VR0007 to R. B. G.) on its Peak Computing Facility at the University of Melbourne, an initiative of the Victorian Government; and an Australian Postgraduate Award from James Cook University (to L. T.).

Potential conflicts of interest. All authors: No reported conflicts.

All authors have submitted the ICMJE Form for Disclosure of Potential Conflicts of Interest. Conflicts that the editors consider relevant to the content of the manuscript have been disclosed.

References

- Hotez PJ, Bethony JM, Diemert DJ, Pearson M, Loukas A. Developing vaccines to combat hookworm infection and intestinal schistosomiasis. *Nat Rev Microbiol* **2010**; 8:814–26.
- Palmer ED. Course of egg output over a 15 year period in a case of experimentally induced necatoriasis americanus, in the absence of hyperinfection. *Am J Trop Med Hyg* **1955**; 4:756–7.
- Albonico M, Smith PG, Ercole E, et al. Rate of reinfection with intestinal nematodes after treatment of children with mebendazole or albendazole in a highly endemic area. *Trans R Soc Trop Med Hyg* **1995**; 89:538–41.
- Loukas A, Bethony J, Brooker S, Hotez P. Hookworm vaccines: past, present, and future. *Lancet Infect Dis* **2006**; 6:733–41.
- Fujiwara RT, Loukas A, Mendez S, et al. Vaccination with irradiated *Ancylostoma caninum* third stage larvae induces a Th2 protective response in dogs. *Vaccine* **2006**; 24:501–9.
- Bethony J, Loukas A, Smout M, et al. Antibodies against a secreted protein from hookworm larvae reduce the intensity of hookworm infection in humans and vaccinated laboratory animals. *FASEB J* **2005**; 19:1743–5.
- Bethony JM, Simon G, Diemert DJ, et al. Randomized, placebo-controlled, double-blind trial of the *Na*-ASP-2 hookworm vaccine in unexposed adults. *Vaccine* **2008**; 26:2408–17.
- Diemert DJ, Pinto AG, Freire J, et al. Generalized urticaria induced by the *Na*-ASP-2 hookworm vaccine: implications for the development of vaccines against helminths. *J Allerg Clin Immunol* **2012**; 130:169–76 e6.
- Zhan B, Santiago H, Keegan B, et al. Fusion of *Na*-ASP-2 with human immunoglobulin Fcγ₁ abrogates histamine release from basophils sensitized with anti-*Na*-ASP-2 IgE. *Parasite Immunol* **2012**; 34:404–11.
- Hazebrouck S, Guillon B, Drumare MF, Paty E, Wal JM, Bernard H. Trypsin resistance of the major peanut allergen Ara h 6 and allergenicity of the digestion products are abolished after selective disruption of disulfide bonds. *Mol Nutr Food Res* **2012**; 56:548–57.
- Koyanagi S, Murakami T, Maeda T, et al. Production-scale purification of the recombinant major house dust mite allergen Der f 2 mutant C8/119S. *J Biosci Bioeng* **2010**; 110:597–601.
- Winkler B, Bolwig C, Seppala U, Spangfort MD, Ebner C, Wiedermann U. Allergen-specific immunosuppression by mucosal treatment with recombinant Ves v 5, a major allergen of *Vespula vulgaris* venom, in a murine model of wasp venom allergy. *Immunology* **2003**; 110:376–85.
- Bungiro R, Cappello M. Twenty-first century progress toward the global control of human hookworm infection. *Curr Infect Dis Rep* **2011**; 13:210–7.
- Hotez PJ, Hawdon JM, Cappello M, et al. Molecular approaches to vaccinating against hookworm disease. *Pediatr Res* **1996**; 40:515–21.
- Bower MA, Constant SL, Mendez S. *Necator americanus*: the *Na*-ASP-2 protein secreted by the infective larvae induces neutrophil recruitment in vivo and in vitro. *Exp Parasitol* **2008**; 118:569–75.
- Osman A, Wang CK, Winter A, et al. Hookworm SCP/TAPS protein structure—A key to understanding host-parasite interactions and developing new interventions. *Biotech Adv* **2012**; 30:652–7.
- Asojo OA, Goud G, Dhar K, et al. X-ray structure of *Na*-ASP-2, a pathogenesis-related-1 protein from the nematode parasite, *Necator americanus*, and a vaccine antigen for human hookworm infection. *J Mol Biol* **2005**; 346:801–14.
- Rieu P, Ueda T, Haruta I, Sharma CP, Arnaout MA. The A-domain of beta 2 integrin CR3 (CD11b/CD18) is a receptor for the hookworm-derived neutrophil adhesion inhibitor NIF. *J Cell Biol* **1994**; 127:2081–91.
- Goud GN, Bottazzi ME, Zhan B, et al. Expression of the *Necator americanus* hookworm larval antigen *Na*-ASP-2 in *Pichia pastoris* and purification of the recombinant protein for use in human clinical trials. *Vaccine* **2005**; 23:4754–64.
- Wang CK, Broder U, Weeratunga SK, Gasser RB, Loukas A, Hofmann A. SBAL: a practical tool to generate and edit structure-based amino acid sequence alignments. *Bioinformatics* **2012**; 28:1026–7.
- Sali A, Blundell TL. Comparative protein modelling by satisfaction of spatial restraints. *J Mol Biol* **1993**; 234:779–815.
- Radaev S, Zou Z, Tolar P, et al. Structural and functional studies of Igalphabeta and its assembly with the B cell antigen receptor. *Structure* **2010**; 18:934–43.
- Ritchie DW, Kozakov D, Vajda S. Accelerating and focusing protein-protein docking correlations using multi-dimensional rotational FFT generating functions. *Bioinformatics* **2008**; 24:1865–73.
- The PyMOL Molecular Graphics System, Version 1.5.0.4 Schrödinger, LLC.
- Langmead B, Trapnell C, Pop M, Salzberg SL. Ultrafast and memory-efficient alignment of short DNA sequences to the human genome. *Genome Biol* **2009**; 10:R25.
- Trapnell C, Williams BA, Pertea G, et al. Transcript assembly and quantification by RNA-Seq reveals unannotated transcripts and isoform switching during cell differentiation. *Nat Biotechnol* **2010**; 28:511–5.
- Mortazavi A, Williams BA, McCue K, Schaeffer L, Wold B. Mapping and quantifying mammalian transcriptomes by RNA-Seq. *Nat Methods* **2008**; 5:621–8.
- Audic S, Claverie JM. The significance of digital gene expression profiles. *Genome Res* **1997**; 7:986–95.
- Benjamini Y, Drai D, Elmer G, Kafkafi N, Golani I. Controlling the false discovery rate in behavior genetics research. *Behav Brain Res* **2001**; 125:279–84.
- Boyle EI, Weng S, Gollub J, et al. GO::TermFinder—open source software for accessing Gene Ontology information and finding significantly enriched Gene Ontology terms associated with a list of genes. *Bioinformatics* **2004**; 20:3710–5.
- Mason L, Tribolet L, Simon A, et al. Probing the equatorial groove of the hookworm protein and vaccine candidate antigen, *Na*-ASP-2. *Int J Biochem Cell Biol* **2014**; 50:146–55.
- Bird DM, Opperman CH. The secret(ion) life of worms. *Genome Biol* **2009**; 10:205.
- Doyle S. Fungal proteomics: from identification to function. *FEMS Microbiol Lett* **2011**; 321:1–9.
- Tang YT, Gao X, Rosa BA, et al. Genome of the human hookworm *Necator americanus*. *Nat Genet* **2014**; 46:261–9.

35. Bethony J, Brooker S, Albonico M, et al. Soil-transmitted helminth infections: ascariasis, trichuriasis, and hookworm. *Lancet* **2006**; 367: 1521–32.
36. Loukas A, Constant SL, Bethony JM. Immunobiology of hookworm infection. *FEMS Immunol Med Microbiol* **2005**; 43:115–24.
37. McSorley HJ, Loukas A. The immunology of human hookworm infections. *Parasite Immunol* **2010**; 32:549–59.
38. Gaze S, McSorley HJ, Daveson J, et al. Characterising the mucosal and systemic immune responses to experimental human hookworm infection. *PLoS Path* **2012**; 8:e1002520.
39. Ferreira I, Smyth D, Gaze S, et al. Hookworm excretory/secretory products induce interleukin-4 (IL-4)+ IL-10+ CD4+ T cell responses and suppress pathology in a mouse model of colitis. *Infect Immun* **2013**; 81:2104–11.
40. Navarro S, Ferreira I, Loukas A. The hookworm pharmacopoeia for inflammatory diseases. *Int J Parasitol* **2013**; 43:225–31.
41. Yang CW, Strong BS, Miller MJ, Unanue ER. Neutrophils influence the level of antigen presentation during the immune response to protein antigens in adjuvants. *J Immunol* **2010**; 185:2927–34.
42. Yang X, Gao X. Role of dendritic cells: a step forward for the hygiene hypothesis. *Cell Mol Immunol* **2011**; 8:12–8.
43. Treanor B. B-cell receptor: from resting state to activate. *Immunology* **2012**; 136:21–7.
44. O'Neill SK, Getahun A, Gauld SB, et al. Monophosphorylation of CD79a and CD79b ITAM motifs initiates a SHIP-1 phosphatase-mediated inhibitory signaling cascade required for B cell anergy. *Immunity* **2011**; 35:746–56.
45. Browne CD, Del Nagro CJ, Cato MH, Dengler HS, Rickert RC. Suppression of phosphatidylinositol 3,4,5-trisphosphate production is a key determinant of B cell anergy. *Immunity* **2009**; 31:749–60.
46. Fujiwara RT, Cancado GG, Freitas PA, et al. *Necator americanus* infection: a possible cause of altered dendritic cell differentiation and eosinophil profile in chronically infected individuals. *PLoS Negl Trop Dis* **2009**; 3:e399.
47. Mortimer K, Brown A, Feary J, et al. Dose-ranging study for therapeutic infection with *Necator americanus* in humans. *Am J Trop Med Hyg* **2006**; 75:914–20.
48. Croese J, Giacomini PR, Navarro S, et al. Trace gluten consumption following experimental hookworm infection restores gluten tolerance in celiac disease. *J Allergy Clin Immunol* **2014**; in press.
49. Hardy IR, Anceriz N, Rousseau F, et al. Anti-CD79 antibody induces B cell anergy that protects against autoimmunity. *J Immunol* **2014**; 192:1641–50.
50. Li Y, Chen F, Putt M, et al. B cell depletion with anti-CD79 mAbs ameliorates autoimmune disease in MRL/lpr mice. *J Immunol* **2008**; 181:2961–72.